Microscopic theory of optic-phonon Raman scattering in quantum-well systems

Kun Huang, Bang-fen Zhu, and Hui Tang
Institute of Semiconductors, Chinese Academy of Sciences, P.O. Box 912, Beijing 100 083, China
and National Laboratory for Superlattices and Related Microstructures, P.O. Box 912, Beijing 100 083, China
(Received 28 July 1989)

A microscopic theory of Raman scattering by optic phonons is worked out systematically, on the basis of recent advances in our knowledge of the electronic and phonon structure of quantum-well systems. With our recently reformulated analytical expressions for the optical modes, explicit expressions for the Raman tensor for the various phonon modes (interfaces as well as bulklike LO and TO modes) are derived, displaying in full the selection rules regarding polarization configuration, phonon parity, and the phonon-scattering mechanisms. As the theoretical results show, certain specific features of quantum-well wave functions are of special importance for a quantitative theory. Thus heavy- and light-hole mixing effects, and the angular momentum state of the excitons, can play a decisive role in determining the predominant scattering channels. These are illustrated by numerically calculated results for various intra- and intersubband scattering channels. Special emphasis has been given to the Fröhlich-interaction-induced scattering, which is dipole allowed in multiple quantum wells owing to the barrier penetrations and heavy- and light-hole mixing.

I. INTRODUCTION

During the past decade, extensive investigations have been carried out on Raman scattering in quantum-well systems.[1-4] The observation of the effect of superlattices on the acoustic phonons in the Raman spectrum was first reported in 1980.[5] The first unambiguous observation of the confined optical modes in GaAs-$Ga_{1-x}Al_xAs$ superlattices was made in 1984.[6] Interface optical modes were discovered in 1985.[7] Several review articles on the subject were given recently by Klein,[1] by Cardona,[2] by Jusserand and Cardona,[3] and by Menéndez,[4] which demonstrated that through Raman scattering studies a basic understanding of the phonon structure of superlattices was established. Besides, resonance scattering has also been exploited in a variety of ways to gain information on the electronic structure and electron-phonon interaction in superlattices.[7-11] On the theoretical side, phonon modes of superlattices have been calculated on various models;[12-18] selection rules regarding phonon symmetry, and the nature of electron-phonon interaction (Fröhlich interaction, or optical deformation potential), for different polarization schemes (polarized or depolarized) have been discussed in relation to experiments.[10,19] Beyond these, however, the theoretical considerations presented for the interpretation of Raman scattering experiments are often fragmentary or speculative.[20] It certainly appears that the lack of a systematically presented microscopic theory of Raman scattering in quantum-well systems is hampering further in-depth investigation on the subject.

The fact that a proper treatment of the subject is not already available is not altogether surprising. As we shall see, it depends on a detailed understanding of the whole complexity of the phonon modes and of the electronic structure of superlattices, which received proper theoretical treatment only in the past few years.[21-26]

In the following, we shall present a systematic microscopic theory for optical-phonon Raman scattering in multiple quantum wells (MQW's). In view of the state of available literature on the subject, we shall endeavor to present our subject in a self-contained manner. Thus we shall start with a description of certain relevant basic features of subband wave functions of quantum-well electrons. Analytical expressions which we have recently derived for the confined bulklike optic-phonon modes in superlattices, and the corresponding electron-phonon interaction, are then introduced. Then explicit formulas for calculating the Raman tensor are derived for Fröhlich interaction as well as for deformation-potential scattering, and for intermediate states consisting of free electron-hole pairs. From the formulas thus derived, the basic selection rules regarding phonon parity and scattering mechanisms in various polarization schemes follow directly. In a separate section, corresponding expressions for the interface modes in superlattices are presented. For exciton-mediated scattering, we shall limit ourselves to comments on certain main features.

The dimensionless Raman tensor for first-order phonon Raman-Stokes scattering is usually expressed as[27,28]

$$\vec{\mathbf{R}}=N^{-3/2}m_e^{-1}\sum_{\alpha,\beta}\frac{\langle 0|\sum_s e^{-i\mathbf{q}_f\cdot\mathbf{r}_s}\mathbf{p}_s|\beta\rangle\langle\beta|H_{EL}|\alpha\rangle\langle\alpha|\sum_s e^{i\mathbf{q}_i\cdot\mathbf{r}_s}\mathbf{p}_s|0\rangle}{(E_0-E_\alpha)(E_0-E_\beta-\hbar\omega_0)}\ , \tag{1}$$

where for simplicity we have explicitly indicated only the electronic states involved in the initial, intermediate, and final states of the whole system (phonon + electron + phonon), namely, $|0\rangle$ for the ground filled valence-band state and $|\alpha\rangle, |\beta\rangle$ for the electron-hole pair states. In the formula H_{EL} is the electron-phonon interaction operator, $\mathbf{p}$ is the single-particle momentum operator, and $\mathbf{q}_i$ and $\mathbf{q}_f$ denote the incident- and scattered-light wave vectors, respectively. E_0 represents the incident photon energy, and $\hbar\omega_0$ is the energy of the emitted phonon. We shall suppose that the superlattice (MWQ's) occupies a total volume of N^3 cells of volume v_0, with N cells along each of the x,y,z directions.

The Raman tensor is made up of terms associated with various intersubband or intrasubband scattering of an electron or a hole. In the following, how such contributions are related to the subband structures will form the central subject for discussion.

The Fröhlich-interaction-induced scattering will be given special emphasis as it is no longer dipole forbidden as in bulk materials, but depends on certain specific features of quantum-well wave functions.

Some calculated results will be given to illustrate certain basic points discussed and to compare with experiments.

II. CERTAIN BASIC FEATURES OF ELECTRON AND HOLE SUBBAND WAVE FUNCTIONS IN QUANTUM WELLS

Our treatment will be restricted to electron and hole states in decoupled quantum wells. The conduction- and valence-band electrons will be treated in the effective-mass approximation. The effective-mass wave function for conduction-band electrons in a single quantum well will be represented as

$$|E\uparrow(\downarrow)\rangle = A^{-1/2} e^{i\mathbf{k}_\parallel\cdot\mathbf{r}} \varphi(z) |\uparrow(\downarrow)\rangle , \tag{2a}$$

where $\uparrow$ and $\downarrow$ are spin functions parallel and antiparallel to the superlattice axis along z. $\mathbf{k}_\parallel$ is the wave vector in the x-y plane. $A=(Na_0)^2$ is the cross-section area. Normally a subband index would be appended; we shall often omit it to reduce formal specifications to a minimum. When we need to specify another state belonging to a different subband, we usually just add an overbar.

To represent a superlattice system, the above quantum-well states will be formally built into the extended Bloch wave functions. Suppose the superlattice has a period of $d=ma_0$ and $N=mL$, so that L is the total number of periods along z; the extended Bloch functions can then be written as

$$|E\uparrow(\downarrow)\rangle = A^{-1/2} e^{i\mathbf{k}_\parallel\cdot\mathbf{r}} L^{-1/2} \times \sum_l e^{ik_z ld} \varphi(z-ld) |\uparrow(\downarrow)\rangle , \tag{2b}$$

where k_z is restricted to the minizone:

$$k_z = 2\pi s/(Ld), \quad -L/2 < s < L/2 .$$

Owing to the fourfold degeneracy of the valence band, the effective-mass wave functions of valence-band states are four-component spinors. In a quantum well, there are a pair of degenerate states for a given $\mathbf{k}_\parallel$ which can be represented as follows:

$$|H^+\rangle = A^{-1/2} e^{i\mathbf{k}_\parallel\cdot\mathbf{r}} \begin{pmatrix} a(k_\parallel,z)\exp(-i\theta) \\ b(k_\parallel,z) \\ c(k_\parallel,z)\exp(i\theta) \\ d(k_\parallel,z)\exp(i2\theta) \end{pmatrix} ,$$

$$|H^-\rangle = A^{-1/2} e^{i\mathbf{k}_\parallel\cdot\mathbf{r}} \begin{pmatrix} d(k_\parallel,z)\exp(-i\theta) \\ c(k_\parallel,z) \\ b(k_\parallel,z)\exp(i\theta) \\ a(k_\parallel,z)\exp(i2\theta) \end{pmatrix} . \tag{3a}$$

Several points need explanation.

With the wave vector $\mathbf{k}_\parallel$ expressed in polar coordinates $(k_\parallel,\theta)$, the component functions a, b, c, and d only depend on $k_\parallel$. The simple explicit dependence on the direction of $\mathbf{k}_\parallel$ through the $e^{in\theta}$ factors reflects symmetry in the x-y plane, where we have used a somewhat modified Kohn-Luttinger Hamiltonian isotropic in the x-y plane. This isotropy approximation simplifies our theoretical presentation and yet does not materially affect our main results (referring specifically to various selection rules following from the Raman tensor).

The pair of degenerate states denoted by $H^\pm$ differ in a reversal of the ordering of the a, b, c, and d functions. These functions are alternately even and odd in z. For definiteness, we designate as the plus state that which has first and third components odd and second and fourth components even. In other words, in the wave functions given in (3), a and c are odd and b and d are even.

A basic feature of the hole subbands in quantum wells is their wave function's behavior at $k_\parallel=0$. For each subband, at $k_\parallel=0$, only one of the four components is nonvanishing and this component remains the dominant component for small $k_\parallel$ (compared with $2\pi/d_0$, d_0 is the quantum-well width). The wave functions with first or fourth components (analogous to $\pm\frac{3}{2}$ spin components) nonvanishing at $k_\parallel=0$ describe heavy holes, and wave functions with second or third components (analogous to $\pm\frac{1}{2}$ spin components) nonvanishing at $k_\parallel=0$ describe light holes. The hole subbands are named heavy- or light-hole bands according to their wave functions at the $k_\parallel=0$ limit. For nonvanishing $k_\parallel$ values, all four components of the wave function are generally nonvanishing. This is usually viewed as a heavy- and light-hole mixing effect from the point of view of $\mathbf{k}\cdot\mathbf{p}$ perturbation as applied to the subbands.

Expressed formally as Bloch functions appropriate to the superlattice, the valence-band states should be written as

$$|H^+\rangle=(LA)^{-1/2}e^{i\mathbf{k}_\parallel\cdot\mathbf{r}} \times\sum_l \begin{bmatrix} a(k_\parallel,z-ld)\exp(-i\theta) \\ b(k_\parallel,z-ld) \\ c(k_\parallel,z-ld)\exp(i\theta) \\ d(k_\parallel,z-ld)\exp(i2\theta) \end{bmatrix} e^{ik_z ld},$$

$$|H^-\rangle=(LA)^{-1/2}e^{i\mathbf{k}_\parallel\cdot\mathbf{r}} \times\sum_l \begin{bmatrix} d(k_\parallel,z-ld)\exp(-i\theta) \\ c(k_\parallel,z-ld) \\ b(k_\parallel,z-ld)\exp(i\theta) \\ a(k_\parallel,z-ld)\exp(i2\theta) \end{bmatrix} e^{ik_z ld}. \quad (3b)$$

III. CONFINED OPTIC-PHONON MODES AND ELECTRON-PHONON INTERACTION

Relatively realistic calculations of the phonon modes in superlattices have become available in recent years.[15–17] However, the use of such numerically calculated phonon modes would make the theoretical treatment of Raman scattering very unwieldy. The often-quoted optical modes derived from the dielectric continuum model[12] would be much more convenient to use. But, as we have shown in a recent paper, they doe not, in fact, correspond to the realistic modes.[18] However, by following clues suggested by results of calculations with a microscopic model closely paralleling the continuum model, we were able to obtain modified expressions for the optic-phonon modes, which are still within the framework of the continuum model, yet agree closely with the modes calculated from the microscopic model (within certain limits to be mentioned later).

As in the usual dielectric continuum treatment, the modified bulklike modes likewise vibrate with the bulk LO and TO frequencies and are confined to either one of the layers constituting the superlattice. Similarly to the case of the electronic wave functions, by introducing a wave number k_z along the superlattice axis to correlate the phases of modes confined to different layers, the modes can be rendered in a form conforming to the periodic structure of the superlattice. Thus the optical displacement vector of a LO mode has been obtained in the following form (with the y axis taken along $\mathbf{k}_\parallel$):

$$\mathbf{u}(\mathbf{r})=(MN^3I_n)^{-1/2}\sum_l \begin{bmatrix} 0 \\ ik_\parallel\Phi_n(z-ld) \\ -\partial\Phi_n(z-ld)/\partial z \end{bmatrix} \times e^{-i(k_\parallel y+k_z ld)}Q^{\mathrm{LO}}(\mathbf{k},n), \quad (4)$$

where $Q^{\mathrm{LO}}(\mathbf{k},n)$ is a complex normal coordinate, related to the creation operator $b^+(\mathbf{k})$ of a $\mathbf{k}$ mode and the annihilation operator $b^-(-\mathbf{k})$ of a $-\mathbf{k}$ mode as follows:

$$Q^{\mathrm{LO}}(\mathbf{k},n)=\left[\frac{\hbar}{2\omega_{\mathrm{LO},n}}\right]^{1/2}[b^+(\mathbf{k})+b^-(-\mathbf{k})].$$

In (4), M represents the reduced mass of the positive and negative ions. $\Phi_n(z)$ describes the various-order confined modes. Their explicit expressions are given by the following even or odd functions:

$$\Phi_n(z)=\cos(n\pi z/w)-(-1)^{n/2},\quad n=2,4,6,\ldots$$

and

$$\Phi_n(z)=\sin(\mu_n\pi z/w)+C_n(z/w),\quad n=3,5,7,\ldots$$

which are supposedly confined to a layer $-w/2<z<w/2$, where $w=d_0+a_0$. The $\Phi_n(z)$ functions are such that they and their derivatives both vanish at the boundaries. It follows from this that μ_n have the following values close to the integers n:

$$\mu_3=2.8606,\quad \mu_5=4.918,\quad \mu_7=6.95,\quad \ldots,$$

and C_n assume the following values close to $+2$ or -2:

$$C_3=1.9523,\quad C_5=-1.983,\quad C_7=1.992,\quad \ldots.$$

I_n is a normalization constant to be determined from $\Phi_n(z)$ by

$$I_n=d^{-1}\int_{-w/2}^{w/2}[k_\parallel^2\Phi_n^2+(\partial\Phi_n/\partial z)^2]dz.$$

TO modes are of two types, polarized parallel and perpendicular to the $\mathbf{k}_\parallel$-z plane, which we shall designate as TO1 and TO2 modes, respectively. The TO1 modes can be expressed in terms of the above-defined $\Phi_n(z)$ functions as follows:

$$\mathbf{u}(\mathbf{r})=(MN^3I_n)^{-1/2}\sum_l \begin{bmatrix} 0 \\ -i\partial\Phi_n(z-ld)/\partial z \\ k_\parallel\Phi_n(z-ld) \end{bmatrix} \times e^{-ik_\parallel y-ik_z ld}Q^{\mathrm{TO1}}(\mathbf{k},n). \quad (5)$$

With the y axis along $k_\parallel$, the TO2 modes are polarized along the x axis. Their displacement vectors are found to be well described by simple sinusoidal standing waves, namely

$$\mathbf{u}(\mathbf{r})=(MN^3)^{-1/2}\left[\frac{2d}{w}\right]^{1/2} \times\sum_l \begin{bmatrix} \Psi_n(z-ld) \\ 0 \\ 0 \end{bmatrix} e^{-ik_\parallel y-ik_z ld}Q^{\mathrm{TO2}}(\mathbf{k},n), \quad (6)$$

where $\Psi_n(z)$ are sinusoidal standing waves confined to a layer $-w/2<z<w/2$:

$$\Psi_n(z)=\begin{cases}\cos(n\pi z/w), & n=1,3,5,\ldots \quad (7a)\\ \sin(n\pi z/w), & n=2,4,6,\ldots. \quad (7b)\end{cases}$$

We have verified that the above analytical expressions for the bulklike optical modes agree closely with the modes calculated from the microscopic model (for zero-phonon dispersion[29]), so long as $k_\parallel<\pi/d_0$. In other words, the phonon wavelength must be larger than the confining length d_0. This is certainly true for phonons

relevant to Raman scattering.

Since the Φ_n functions correspond to wave vectors $n\pi/d_0$, one sees from (4) and (5) that for the relevant long-wavelength phonon modes the LO modes are polarized essentially along the z axis and the TO1 modes are polarized essentially along the y axis. It is interesting to note that the polarization features of these LO and TO1 modes differ radically from the case of bulk materials. Thus, here the LO modes are polarized perpendicular rather than parallel to the really operative wave vector $\mathbf{k}_\parallel$ (k_z is purely formal), and the TO1 modes are polarized parallel rather than perpendicular to the wave vector $\mathbf{k}_\parallel$.

Next, we derive explicit expressions for the electron-phonon scattering matrix element required to calculate the Raman tensor; first for deformation-potential interaction, then for Fröhlich interaction.

The deformation-potential interaction arises from the perturbation of the lattice-periodic potential by the optic-phonon modes. A long-wavelength optical mode causes a "local" change (in the macroscopic sense) in the lattice-periodic potential, essentially the same as that due to a uniform relative displacement between the positive and negative ions. In linear approximations, the change of the lattice-periodic potential can be represented as

$$\mathbf{u}\cdot\mathbf{U}(\mathbf{r})=u_x U_x(\mathbf{r})+u_y U_y(\mathbf{r})+u_z U_z(\mathbf{r}) .$$

The effective-mass wave functions are in the nature of envelope functions. In forming the matrix elements of the deformation potential, we should, of course, start with using the proper wave functions, which are the effective-mass functions multiplied by the corresponding band-edge functions. In evaluating such matrix elements, the well-known practice is to neglect variations of the slowly varying factors (in the present case, the effective-mass functions and the phonon displacements) over a lattice cell, so that the fast varying factor with the lattice periodicity can be replaced by their integral average. Thus the deformation-potential interaction can be characterized by such integral averages of the functions U_x, U_y, U_z taken between the band-edge functions, which can be represented as

$$\langle s|U_j|t\rangle=v_0^{-1}\int d\mathbf{r}\, u_s^* U_j u_t , \tag{8}$$

where the u_s, u_t functions represent normalized band-edge functions of the bands concerned. For hole scattering, the fourfold-degenerate valence-band-edge functions can be represented as follows:

$$\begin{aligned}
u_{3/2}&=2^{-1/2}(X+iY)|\uparrow\rangle ,\\
u_{1/2}&=i6^{-1/2}[(X+iY)|\downarrow\rangle-2Z|\uparrow\rangle] ,\\
u_{-1/2}&=6^{-1/2}[(X-iY)|\uparrow\rangle+2Z|\downarrow\rangle] ,\\
u_{-3/2}&=i2^{-1/2}(X-iY)|\downarrow\rangle ,
\end{aligned} \tag{9}$$

where X, Y, Z are spatial functions transforming as x, y, z under the T_d point-group operators. It can be readily proved by the usual symmetry analysis that the only nonvanishing integrals of the U_x, U_y, U_z functions of the deformation potential taken between the X, Y, Z functions are the following:

$$\begin{aligned}
\langle Y|U_x|Z\rangle&=\langle Z|U_x|Y\rangle=\langle Z|Y_y|X\rangle\\
&=\langle X|U_y|Z\rangle\\
&=\langle X|U_z|Y\rangle\\
&=\langle Y|U_z|X\rangle=C ,
\end{aligned}$$

where C expresses the common value of the nonvanishing integrals. Making use of this result, one readily finds that the integral averages taken between the four band-edge functions (9) can be expressed in matrix form as follows:

$$\langle i|U_x|j\rangle=\frac{C}{\sqrt{3}}\begin{pmatrix} 0 & -1 & 0 & 0\\ -1 & 0 & 0 & 0\\ 0 & 0 & 0 & 1\\ 0 & 0 & 1 & 0\end{pmatrix} , \tag{10}$$

$$\langle i|U_y|j\rangle=\frac{C}{\sqrt{3}}\begin{pmatrix} 0 & -i & 0 & 0\\ i & 0 & 0 & 0\\ 0 & 0 & 0 & i\\ 0 & 0 & -i & 0\end{pmatrix} , \tag{11}$$

$$\langle i|U_z|j\rangle=\frac{C}{\sqrt{3}}\begin{pmatrix} 0 & 0 & -i & 0\\ 0 & 0 & 0 & -i\\ i & 0 & 0 & 0\\ 0 & i & 0 & 0\end{pmatrix} . \tag{12}$$

Owing to symmetry, the integrals of the U functions between conduction-band-edge functions vanish.

On the basis of these deformation potentials between the band-edge functions, explicit expressions for the phonon-scattering matrix elements H_{EL} can be derived. For this purpose, α and β have to be more explicitly specified. α stands for an electron state $E(\mathbf{k}')$ paired with a hole state $H^{\pm}(\mathbf{k})$ and is accordingly represented by a Slater determinant of the filled valence band, in which the hole wave function $H^{\pm}(\mathbf{k})$ is replaced by the electron wave function $E(\mathbf{k}')$. Similarly, β will stand for an electron state $\bar{E}(\mathbf{k}'')$ paired with a hole state $\bar{H}^{\pm}(\mathbf{k}'')$ and is represented by a corresponding Slater determinant. However, in specifying these states, their wave vectors will be explicitly indicated within brackets as in the above only when considered really necessary.

As the electron-phonon interaction is in the nature of single-particle interaction, its matrix elements between the β and α determinantal wave functions can be straightforwardly worked out in terms of single-particle matrix elements, namely

$$\begin{aligned}
\langle\beta|H_{EL}|\alpha\rangle=&\,\delta_{H^{\pm},\bar{H}^{\pm}}\langle\bar{E}|H_{EL}|E\rangle\\
&-\delta_{E,\bar{E}}\langle H^{\pm}|H_{EL}|\bar{H}^{\pm}\rangle .
\end{aligned} \tag{13}$$

Consider first the LO modes. As noted earlier, for the modes relevant to Raman scattering, they are polarized essentially along the z axis. So for deformation-potential scattering, we need only consider the z displacement from (4), namely

$$u_z(\mathbf{r})=\left[\frac{\hbar}{2M\omega_{\mathrm{LO}}N^3I_n}\right]^{1/2}\sum_l[-\partial\Phi_n(z-ld)/\partial z]\times e^{-ik_{\parallel}^0 y-ik_z^0 ld}\times[b^+(\mathbf{k}^0)+b^-(-\mathbf{k}^0)]\ , \tag{14}$$

where the phonon wave vector is specified as $\mathbf{k}^0$, so as to distinguish it from the wave vectors of the electrons or holes. When we consider forming a matrix element $\langle H^+|H_{EL}|\bar{H}^+\rangle$ of the deformation potential caused by u_z as given in (14) between hole wave functions $H^+,\bar{H}^+$ of the form (3a), they are all sums of terms with respective indices (say, l, l', and l'') running over the L periods. On integration, clearly only their corresponding terms (i.e., $l=l'=l''$ terms) overlap and make a nonvanishing contribution. Moreover, these contributions are readily seen to be identical apart from a phase factor $\exp[i(-k_z^0-k_z+k_z'')ld]$, which, when summed over l, just gives a δ function expressing conservation of the total wave vector:

$$k_z''=k_z+k_z^0$$

along the z axis. Apart from this, writing down the scattering matrix element for LO-phonon emission according to (13), with the help of (14), (12), and (3a) is straightforward, giving

$$\langle\beta|H_{EL}|\alpha\rangle_{\mathrm{LO}}=i\delta(\mathbf{k}''-\mathbf{k}-\mathbf{k}^0)D(N^3I_n)^{-1/2}(-\langle a|\Phi_n'|\bar{c}\rangle e^{2i\theta}-\langle b|\Phi_n'|\bar{d}\rangle e^{2i\theta}+\langle c|\Phi_n'|\bar{a}\rangle e^{-2i\theta}+\langle d|\Phi_n'|\bar{b}\rangle e^{-2i\theta})\delta_{E,\bar{E}}\ , \tag{15}$$

where the deformation potential is characterized by

$$D=\frac{C}{\sqrt{3}}\left[\frac{\hbar}{2M\omega_{\mathrm{LO}}}\right]^{1/2}$$

with the dimension of energy and Φ_n' represents the derivative of the function $\Phi_n(z)$.

For the TO1 modes given by (5), we need only consider its y displacement:

$$u_y(\mathbf{r})=\left[\frac{\hbar}{2M\omega_{\mathrm{TO}}N^3I_n}\right]^{1/2}\sum_l[-i\partial\Phi_n(z-ld)/\partial z]e^{-ik_{\parallel}^0 y-ik_z^0 ld}[b^+(\mathbf{k}^0)+b^-(-\mathbf{k}^0)]\ . \tag{16}$$

The only essential difference from the LO case is that the relevant deformation potential is now (11) for y displacement. Thus we obtain for TO1 phonon emission the scattering matrix element:

$$\langle\beta|H_{EL}|\alpha\rangle_{\mathrm{TO1}}=\delta(\mathbf{k}''-\mathbf{k}-\mathbf{k}^0)D(N^3I_n)^{-1/2}(\omega_{\mathrm{LO}}/\omega_{\mathrm{TO}})^{1/2}(\langle a|\Phi_n'|\bar{b}\rangle e^{i\theta}-\langle b|\Phi_n'|\bar{a}\rangle e^{-i\theta}-\langle c|\Phi_n'|\bar{d}\rangle e^{i\theta}+\langle d|\Phi_n'|\bar{c}\rangle e^{-i\theta})\delta_{E,\bar{E}}\ . \tag{17}$$

The TO2 modes given in (6) have only the x component. With a deformation potential due to x displacement (10), we obtain for TO2 phonon emission the following scattering matrix element:

$$\langle\beta|H_{\mathrm{EL}}|\alpha\rangle_{\mathrm{TO2}}=\delta(\mathbf{k}''-\mathbf{k}-\mathbf{k}^0)DN^{-3/2}(2d/w)^{1/2}(\omega_{\mathrm{LO}}/\omega_{\mathrm{TO}})^{1/2}(\langle a|\Psi_n|\bar{b}\rangle e^{i\theta}+\langle b|\Psi_n|\bar{a}\rangle e^{-i\theta}-\langle c|\Psi_n|\bar{d}\rangle e^{i\theta}-\langle d|\Psi_n|\bar{c}\rangle e^{-i\theta})\delta_{E,\bar{E}}\ . \tag{18}$$

It should be noted that in writing down the $e^{in\theta}$ factors in the above matrix elements, we have neglected the small difference between $\mathbf{k}(k,\theta)$ and $\mathbf{k}''(k'',\theta'')$ (they differ by the phonon wave vector $\mathbf{k}^0$). Strictly speaking, one should have distinguished between $e^{in\theta}$ and $e^{in\theta'}$ corresponding, respectively, to the H^+ and $\bar{H}^+$ holes, whereas in the above matrix elements, such differences are ignored.

In the preceding, matrix elements have been written down only for $H^+\rightarrow\bar{H}^+$ scattering. Similar matrix elements for $H^+\rightarrow\bar{H}^-$, $H^-\rightarrow\bar{H}^+$, and $H^-\rightarrow\bar{H}^-$ scatterings can be directly obtained by reversing the ordering of $\bar{a},\bar{b},\bar{c},\bar{d}$ or a,b,c,d, or both in the above formulas.

As in bulk materials, the LO modes are associated with an electrostatic field. The electrostatic potential corresponding to the LO mode given in (4) is given by

$$V(\mathbf{r})=-(N^3v_0I_n)^{-1/2}[4\pi(\omega_{\mathrm{LO}}^2-\omega_{\mathrm{TO}}^2)/\epsilon_\infty]^{1/2}\sum_l\Phi_n(z-ld)e^{-ik_{\parallel}^0 y-ik_z^0 ld}Q^{\mathrm{LO}}(\mathbf{k},n)\ . \tag{19}$$

The Fröhlich interaction with electrons is just $-eV(\mathbf{r})$. By Fröhlich interaction, the LO modes can scatter either an electron or a hole, and the matrix elements can be worked out according to (13). As in the present case the electron-phonon interaction, unlike the deformation potential, can be considered as slowly varying, so in the integration the band-edge functions only provide an orthogonality factor between distinct band edges. We obtain directly from $V(\mathbf{r})$ given in (19) and the effective-mass wave functions (2b) and (3b) that

$$\langle\beta|H_{EL}|\alpha\rangle_{\mathrm{LO},F}=e(N^3v_0I_n)^{-1/2}[2\pi(\omega_{\mathrm{LO}}^2-\omega_{\mathrm{TO}}^2)/\epsilon_\infty]^{1/2}(\hbar/\omega_{\mathrm{LO}})^{1/2}$$
$$\times[\delta(-\mathbf{k}'''+\mathbf{k}'-\mathbf{k}^0)\langle\bar{\varphi}|\Phi_n|\varphi\rangle\delta_{H^\pm\bar{H}^\pm}$$
$$-\delta(\mathbf{k}''-\mathbf{k}-\mathbf{k}^0)(\langle a|\Phi_n|\bar{a}\rangle+\langle b|\Phi_n|\bar{b}\rangle+\langle c|\Phi_n|\bar{c}\rangle+\langle d|\Phi_n|\bar{d}\rangle)\delta_{E,\bar{E}}] . \tag{20}$$

IV. PHOTON INTERACTION MATRIX ELEMENTS AND BASIC WAVE-VECTOR RELATIONS

The photon interaction matrix element,

$$\langle\alpha|\sum_s e^{i\mathbf{q}_i\cdot\mathbf{r}_s}\mathbf{p}_s|0\rangle ,$$

between the α-determinant wave function and the Slater determinant for the filled valence band reduces simply to the single-particle matrix element

$$\langle E(\mathbf{k}')\uparrow\downarrow|e^{-i\mathbf{q}_i\cdot\mathbf{r}}\mathbf{p}|H^\pm(\mathbf{k})\rangle ,$$

where, for later convenience, we have explicitly indicated that the electron state may have $\uparrow$ or $\downarrow$ spin, just as the hole may be H^+ or H^-.

In working out the above matrix element, the electron and hole functions E and $H^\pm$ as given in (2b) and (3b) are both sums of the terms with respective indices (e.g., l,l') running over the L periods. On integration, clearly only mutually corresponding terms (i.e., $l=l'$) overlap and make a contribution; moreover, it is readily seen that these contributions are identical apart from a phase factor of the form

$$\exp[i(-k_z'+q_{iz}+k_z)ld] ,$$

which, on summing over l, gives just a factor

$$\delta(-k_z'+q_{iz}+k_z) , \tag{21}$$

expressing conservation of the wave vector along the z direction. In this connection, we should note that the hole should be associated with $-\mathbf{k}$. Apart from the δ factor (21), the matrix element is reduced to that for a single quantum well, to be worked out with the simple quantum-well wave functions given in (2) and (3) multiplied by the appropriate band-edge functions.

As before, out of $H^\pm$ we need only to work out explicitly the case of H^+; the result can be easily carried over to the H^- case by reversing the order of a,b,c,d.

Writing the integrals of $\mathbf{p}$ taken between the band-edge functions as

$$\langle\uparrow\downarrow|\mathbf{p}|\tfrac{3}{2}\rangle=v_0^{-1}\int_{v_0}d\mathbf{r}\,u_0^*\uparrow\downarrow\mathbf{p}u_{3/2} ,$$

etc., we obtain, on further integration over the slowly varying factors,

$$\langle E(\mathbf{k}')\uparrow\downarrow|e^{i\mathbf{q}_i\cdot\mathbf{r}}\mathbf{p}|H^+(\mathbf{k})\rangle=\delta(-\mathbf{k}'+\mathbf{q}_i+\mathbf{k})[\langle\uparrow\downarrow|\mathbf{p}|\tfrac{3}{2}\rangle(a)e^{-i\theta}$$
$$+\langle\uparrow\downarrow|\mathbf{p}|\tfrac{1}{2}\rangle(b)+\langle\uparrow\downarrow|\mathbf{p}|-\tfrac{1}{2}\rangle(c)e^{i\theta}+\langle\uparrow\downarrow|\mathbf{p}|-\tfrac{3}{2}\rangle(d)e^{2i\theta}] . \tag{22}$$

In obtaining (22), the integration over the x-y plane just supplements (21) to give the δ function. The z integration reduces to essentially overlap integrals between the electron and hole wave functions apart from a phase factor e^{iq_zz}. As the photon wavelength is much larger than the quantum-well widths, this factor will be set equal to 1 (dipole approximation in the superlattice). For the overlap integrals, we have introduced the simplified notations

$$(a)\equiv\int_{-d/2}^{d/2}\varphi^*(z)a(z)dz ,$$

etc. The photon interaction matrix element

$$\langle 0|\sum_s e^{i\mathbf{q}_f\cdot\mathbf{r}_s}\mathbf{p}_s|\beta\rangle=\langle\bar{H}^\pm(\mathbf{k}'')|e^{-i\mathbf{q}_f\cdot\mathbf{r}}\mathbf{p}|\bar{E}(\mathbf{k}''')\uparrow\downarrow\rangle$$

can be worked out in an entirely similar manner, with the result

$$\langle\bar{H}^+(\mathbf{k}''')|e^{-i\mathbf{q}_f\cdot\mathbf{r}}\mathbf{p}|\bar{E}(\mathbf{k}''')\uparrow\downarrow\rangle=\delta(-\mathbf{k}_f''-\mathbf{q}_f+\mathbf{k}''')(\langle\tfrac{3}{2}|\mathbf{p}|\uparrow\downarrow\rangle(\bar{a}^*)e^{i\theta}$$
$$+\langle\tfrac{1}{2}|\mathbf{p}|\uparrow\downarrow\rangle(\bar{b}^*)+\langle-\tfrac{1}{2}|\mathbf{p}|\uparrow\downarrow\rangle(\bar{c}^*)e^{-i\theta}$$
$$+\langle-\tfrac{3}{2}|\mathbf{p}|\uparrow\downarrow\rangle(\bar{d}^*)e^{-2i\theta}) . \tag{23}$$

TABLE I. Integral of **p** between valence-band-edge functions and conduction-band-edge functions.

	Electron spin up				Electron spin down			
i	$\frac{3}{2}$	$\frac{1}{2}$	$-\frac{1}{2}$	$-\frac{3}{2}$	$\frac{3}{2}$	$\frac{1}{2}$	$-\frac{1}{2}$	$-\frac{3}{2}$
$\langle u_0\|p_x\|i\rangle$	$P/\sqrt{2}$	0	$P/\sqrt{6}$	0	0	$iP/\sqrt{6}$	0	$iP/\sqrt{2}$
$\langle u_0\|p_y\|i\rangle$	$iP/\sqrt{2}$	0	$-iP/\sqrt{6}$	0	0	$-P/\sqrt{6}$	0	$P/\sqrt{2}$
$\langle u_0\|p_z\|i\rangle$	0	$-iP\sqrt{2/3}$	0	0	0	0	$P\sqrt{2/3}$	0

The meaning of the symbols for the overlap integrals is readily inferred, namely

$$(a^*)=\int_{-d/2}^{d/2} dz\, a^*(z)\varphi(z), \text{ etc .}$$

Taking account of the symmetry of the valence-band-edge functions (9) and conduction-band-edge functions $u_0\uparrow, u_0\downarrow$, the above band-edge integrals of **p** are easily expressed in terms of the single nonvanishing parameter:

$$P=v_0^{-1}\int_{v_0} d\mathbf{r}\, u_0 p_x X = v_0^{-1}\int_{v_0} d\mathbf{r}\, u_0 p_y Y = v_0^{-1}\int_{v_0} d\mathbf{r}\, u_0 p_z Z$$

as given in Table I.

In the preceding, we derived the individual matrix elements in the Raman tensor. The successive transition matrix elements for $0\to\alpha$, $\alpha\to\beta$, and $\beta\to 0$ each contains a δ function, expressing conservation of total wave vector. Combining these three δ functions contained in Eqs. (22), (23), and (20) [or (18), (17), and (15)], we finally have a basic wave-vector equation, relating the wave vector of the phonon, $\mathbf{k}^0$, to those of the incident and scattered photons, $\mathbf{q}_i$ and $\mathbf{q}_f$:

$$\mathbf{q}_f=\mathbf{q}_i-\mathbf{k}^0 . \tag{24}$$

V. SYMMETRIZED RAMAN NUMERATOR (SRN) AND SELECTION RULES

Apart from establishing the basic wave-vector equation (24), in the calculation of the Raman tensor the photon and phonon wave vectors can be considered as negligibly small (we have already made this approximation in writing down the phonon scattering and photon interaction matrix elements). In other words, the differences between the wave vectors **k**, **k'**, **k''**, and **k'''** for the intermediate electron and hole states can be ignored. Thus in enumerating the intermediate states in the Raman tensor, apart from covering the various electron and hole subbands, there is only a single **k** to be summed over. With this sum over **k** expressed as an integral in **k** space within the minizone in the usual way, we can express the Raman tensor as

$$\begin{aligned}\overleftrightarrow{\mathbf{R}}=&\left[\frac{a_0}{2\pi}\right]^2 m_e^{-1}\sum_{H,\bar{H}}\sum_{E,\bar{E}}\int_0^{k_M} dk_\parallel\, k_\parallel\{[E_0-EH(k_\parallel)][E_0-\overline{EH}(k_\parallel)-\hbar\omega_0]\}^{-1}\\ &\times\Bigg\{\Sigma^{\pm}\overline{\Sigma}^{\pm}\int d\theta[\langle\bar{H}^+|\mathbf{p}|\bar{E}\uparrow\rangle(-\delta_{E,\bar{E}}\langle H^+|H_{EL}|\bar{H}^+\rangle\\ &+\delta_{H^+,\bar{H}^+}\langle\bar{E}|H_{EL}|E\rangle)\langle E\uparrow|\mathbf{p}|H^+\rangle\\ &+\langle\bar{H}^+|\mathbf{p}|\bar{E}\downarrow\rangle(-\delta_{E,\bar{E}}\langle H^+|H_{EL}|\bar{H}^+\rangle\\ &+\delta_{H^+,\bar{H}^+}\langle\bar{E}|H_{EL}|E\rangle)\langle E\downarrow|\mathbf{p}|H^+\rangle]\Bigg\},\end{aligned} \tag{25}$$

where $EH(k_\parallel)$ and $\overline{EH}(k_\parallel)$ have been introduced to represent the excitation energies creating the electron-hole pairs $E(\mathbf{k}),H(\mathbf{k})$ and $\bar{E}(\mathbf{k}),\bar{H}(\mathbf{k})$. $\Sigma^{\pm}$ is used to indicate that the state shown as H^+ should be summed over the degenerate pair $H^{\pm}$, and $\overline{\Sigma}^{\pm}$ indicates the same with the barred states. In the formula, for later convenience, the sum over the spin-degenerate electron states is explicitly displayed, where we have made use of the fact that the phonon scattering does not change the electron spin. In conformity with the isotropy approximation in the x-y plane, the **k**-space integration in the x-y plane is carried out in a circular region of radius $\mathbf{k}_M$ to be determined by

$$\left[\frac{a_0}{2\pi}\right]^2\int_0^{k_M} 2\pi dk_\parallel\, k_\parallel=1 .$$

The trio of matrix elements in the numerator of the Raman tensor is the basic element in constructing the Raman tensor; for want of a better name, we shall just label it the Raman numerator (RN). In expression (25) for the Raman tensor, the sum over the intermediate state is so ordered that the second factor enclosed in brackets is just a sum of the Raman numerator over intermediate states which are mutually degenerate. The degeneracies express the symmetry inherent in the electronic structure. Hence the sum of the Raman numerator over such de-

generate states will show up the symmetry properties of the Raman tensor and will be called the symmetrized Raman numerator (SRN). The rest of this section is devoted to working out the SRN for various polarization configurations.

Following the usual convention for labeling polarization configurations, $\mathcal{N}_{SR}(ij)$ will be used to denote the SRN for incident light polarized along the i axis and scattered light polarized along the j axis. Thus $\mathcal{N}_{SR}(ij)$ can be represented as

$$\mathcal{N}_{SR}(ij)=\sum^{\pm}\overline{\sum}^{\pm}\frac{1}{2\pi}\int d\theta\,[ji](-\delta_{E,\bar{E}}\langle H^{+}|H_{EL}|\bar{H}^{+}\rangle+\delta_{H^{+},\bar{H}^{+}}\langle\bar{E}|H_{EL}|E\rangle)\ , \tag{26}$$

where we have introduced the notation

$$[ji]=\langle\bar{H}^{+}|p_j|\bar{E}\uparrow\rangle\langle E\uparrow|p_i|H^{+}\rangle+\langle\bar{H}^{+}|p_j|\bar{E}\downarrow\rangle\langle E\downarrow|p_i|H^{+}\rangle\ . \tag{27}$$

Consider first polarized scattering, namely, incident and scattered photons similarly polarized. With the help of Eqs. (22) and (23), and the values in Table I, we find for the polarized configurations

$$[xx]=|P|^2\left\{\tfrac{1}{2}((\bar{a}^{*})(a)+(\bar{d}^{*})(d)+\tfrac{1}{3}(\bar{b}^{*})(b)+\tfrac{1}{3}(\bar{c}^{*})(c))\right.$$
$$\left.+\frac{e^{2i\theta}}{2\sqrt{3}}((\bar{a}^{*})(c)+(\bar{b}^{*})(d))+\frac{e^{-2i\theta}}{2\sqrt{3}}((\bar{c}^{*})(a)+(\bar{d}^{*})(b))\right\}\ , \tag{28}$$

$$[yy]=|P|^2\left\{\tfrac{1}{2}((\bar{a}^{*})(a)+(\bar{d}^{*})(d)+\tfrac{1}{3}(\bar{b}^{*})(b)+\tfrac{1}{3}(\bar{c}^{*})(c))\right.$$
$$\left.-\frac{e^{2i\theta}}{2\sqrt{3}}((\bar{a}^{*})(c)+(\bar{b}^{*})(d))-\frac{e^{-2i\theta}}{2\sqrt{3}}((\bar{c}^{*})(a)+(\bar{d}^{*})(b))\right\}\ , \tag{29}$$

$$[zz]=\tfrac{2}{3}|P|^2((\bar{b}^{*}))(b)+(\bar{c}^{*})(c))\ . \tag{30}$$

To obtain the SRN according to (26), these have to be combined with the phonon scattering matrix element, then summed over the degenerate states.

Consider first the case of Fröhlich scattering by the LO modes. Each polarization configuration has to be dealt with separately.

For the polarization (xx), as the Fröhlich scattering matrix element (20) does not depend on θ, the $e^{\pm 2i\theta}$ terms in $[xx]$ drop out on θ integration. Carrying out the sums $\sum^{\pm}\overline{\sum}^{\pm}$ according to (26) just means summing over expressions obtained by reversing the order of a,b,c,d and the order of $\bar{a},\bar{b},\bar{c},\bar{d}$. For electron scattering, the sum $\sum^{\pm}\overline{\sum}^{\pm}$ with $\delta_{H^{\pm},\bar{H}^{\pm}}$ just gives a factor of 2. For hole scattering, as the electron wave function remains unchanged, for the products of overlap integrals not to vanish altogether, the parities of the H and $\bar{H}$ hole components must be mutually matched. This means that in carrying out the sum $\sum^{\pm}\overline{\sum}^{\pm}$, we need only consider simultaneously reversing the order of a,b,c,d and $\bar{a},\bar{b},\bar{c},\bar{d}$, which does not change either $[xx]$ (excluding the $e^{\pm 2i\theta}$ terms) or the hole scattering matrix element (20). So $\sum^{\pm}\overline{\sum}^{\pm}$ again just doubles the value. Thus from (28) and (20), we get

$$\mathcal{N}_{SR}^{\mathrm{LO},F}(xx)=e|P|^2(N^3v_0I_n)^{-1/2}[4\pi(\omega_{\mathrm{LO}}^2-\omega_{\mathrm{TO}}^2)/\epsilon_\infty]^{1/2}(\hbar/2\omega_{\mathrm{LO}})^{1/2}$$
$$\times[\delta_{H,\bar{H}}\langle\bar{\varphi}|\Phi_n|\varphi\rangle-\delta_{E,\bar{E}}(\langle a|\Phi_n|\bar{a}\rangle+\langle b|\Phi_n|\bar{b}\rangle+\langle c|\Phi_n|\bar{c}\rangle+\langle d|\Phi_n|\bar{d}\rangle)]$$
$$\times[(\bar{a}^{*})(a)+(\bar{d}^{*})(d)+\tfrac{1}{3}((\bar{b}^{*})(b)+(\bar{c}^{*})(c))]\ , \tag{31}$$

where superscripts have been appended to indicate the phonon mode and the nature of interaction (F for Fröhlich).

$[yy]$ differs from $[xx]$ only in a change of sign of the $e^{\pm 2i\theta}$ terms, which, as we have seen, are irrelevant to the result. So we have

$$\mathcal{N}_{SR}^{\mathrm{LO},F}(yy)=\mathcal{N}_{SR}^{\mathrm{LO},F}(xx)\ . \tag{32}$$

Working out the case of (zz) follows an entirely similar line of argument, and the following result is obtained:

$$\mathcal{N}_{SR}^{\mathrm{LO},F}(zz)=\tfrac{4}{3}e|P|^2(N^3v_0I_n)^{-1/2}[4\pi(\omega_{\mathrm{LO}}^2-\omega_{\mathrm{TO}}^2)/\epsilon_\infty]^{1/2}(\hbar/2\omega_{\mathrm{LO}})^{1/2}$$
$$\times[\delta_{H\bar{H}}\langle\bar{\varphi}|\Phi_n|\varphi\rangle-\delta_{E,\bar{E}}(\langle a|\Phi_n|\bar{a}\rangle+\langle b|\Phi_n|\bar{b}\rangle+\langle c|\Phi_n|\bar{c}\rangle+\langle d|\Phi_n|\bar{d}\rangle)](\bar{b}^{*})(b)+(\bar{c}^{*})(c))\ . \tag{33}$$

It is to be noted that the results (31)–(33) imply that $\Phi_n(z)$ must be even in z. For the expressions not to vanish, φ and $\bar{\varphi}$, as well as the corresponding hole components, must have the same parity; the matrix elements of $\Phi_n(z)$ would thus all vanish for $\Phi_n(z)$ odd in z.

In these polarized configurations, all deformation-potential scatterings are not effective. This is immediately evident with the TO1 and TO2 phonon modes, for their scattering matrix elements given in (17) and (18) contain only terms with $e^{\pm i\theta}$. When they are multiplied to $[xx]$, $[yy]$, and $[zz]$, as given in (28)–(30), the resulting terms all contain $e^{\pm i\theta}$ or $e^{\pm 3i\theta}$ and hence vanish on θ integration.

With the case of LO deformation-potential scattering, we find that the scattering matrix element (15) contains only terms with $e^{\pm 2i\theta}$ factors. This multiplied to $[zz]$, which does not depend on θ, clearly vanishes on θ integration. The same matrix elements multiplied to $[xx]$ and $[yy]$ gives, apart from terms containing $e^{in\theta}$ (n denotes an integer not equal to 0), the following:

$$\pm iD|P|^2(12N^3I_n)^{-1/2}[-(\langle a|\Phi_n'|\bar{c}\rangle+\langle b|\Phi_n'|\bar{d}\rangle)\times((\bar{c}\,^*)(a)+(\bar{d}\,^*)(b))+(\langle c|\Phi_n'|\bar{a}\rangle+\langle d|\Phi_n'|\bar{b}\rangle)\times((\bar{a}\,^*)(c)+(\bar{b}\,^*)(d))]\ .$$

It is readily verified that when we reverse both the order of a,b,c,d and $\bar{a},\bar{b},\bar{c},\bar{d}$, the above expression just changes its sign. Therefore the sum $\sum^{\pm}\overline{\sum}^{\pm}$ leads to a zero result.

Next we consider the depolarized configurations. With the help of (22), (23), and the values in Table I, we find

$$[yz]=3^{-1/2}|P|^2[-e^{i\theta}((\bar{a}\,^*)(b)+3^{-1/2}(\bar{b}\,^*)(c))+e^{-i\theta}((\bar{d}\,^*)(c)+3^{-1/2}(\bar{c}\,^*)(b))]\ , \tag{34}$$

$$[zy]=3^{-1/2}|P|^2[-e^{i\theta}((\bar{b}\,^*)(a)+3^{-1/2}(\bar{c}\,^*)(b))+e^{-i\theta}((\bar{c}\,^*)(d)+3^{-1/2}(\bar{b}\,^*)(c))]\ , \tag{35}$$

$$[xz]=-i3^{-1/2}|P|^2[e^{i\theta}((\bar{a}\,^*)(b)+3^{-1/2}(\bar{b}\,^*)(c))+e^{-i\theta}((\bar{d}\,^*)(c)+3^{-1/2}(\bar{c}\,^*)(b))]\ , \tag{36}$$

$$[zx]=i3^{-1/2}|P|^2[e^{i\theta}((\bar{c}\,^*)(d)+3^{-1/2}(\bar{b}\,^*)(c))+e^{-i\theta}((\bar{b}\,^*)(a)+3^{-1/2}(\bar{c}\,^*)(b))]\ , \tag{37}$$

$$[xy]=\frac{i}{2}|P|^2[(\bar{a}\,^*)(a)-(\bar{d}\,^*)(d)+\tfrac{1}{3}((\bar{b}\,^*)(b)-(\bar{c}\,^*)(c))-3^{-1/2}e^{2i\theta}((\bar{a}\,^*)(c)+(\bar{b}\,^*)(d))+3^{-1/2}e^{-2i\theta}((\bar{c}\,^*)(a)+(\bar{d}\,^*)(b))]\ , \tag{38}$$

$$[yx]=\frac{i}{2}|P|^2[-(\bar{a}\,^*)(a)+(\bar{d}\,^*)(d)-\tfrac{1}{3}((\bar{b}\,^*)(b)-(\bar{c}\,^*)(c))-3^{-1/2}e^{2i\theta}((\bar{a}\,^*)(c)+(\bar{b}\,^*)(d))+3^{-1/2}e^{-2i\theta}((\bar{c}\,^*)(a)+(\bar{d}\,^*)(b))]\ . \tag{39}$$

The Fröhlich interaction of the LO mode is not effective in any of the depolarized configurations. This is obvious with $[yz]$, $[zy]$, $[zx]$, and $[xz]$, as they contain only $e^{\pm i\theta}$ terms and the Fröhlich scattering matrix element is independent of θ. $[xy]$ and $[yx]$ do contain the following terms independent of θ:

$$\pm\frac{i}{2}|P|^2[(\bar{a}\,^*)(a)-(\bar{d}\,^*)(d)+\tfrac{1}{3}((\bar{b}\,^*)(b)-(\bar{c}\,^*)(c))]\ .$$

But when we reverse both a,b,c,d and $\bar{a},\bar{b},\bar{c},\bar{d}$, the expression just changes its sign, while the Fröhlich scattering matrix element remains unchanged. It follows that on carrying out the sum $\sum^{\pm}\overline{\sum}^{\pm}$, we shall obtain terms that exactly cancel.

The two-LO-phonon Fröhlich scattering is also forbidden in the depolarized configuration, even when the heavy- and light-hole mixing is taken into account. This point was not appropriately noted in a recently published paper,[30] where the ignored θ integration would have yielded a zero result.

The LO deformation-potential scattering matrix element (15) contains only $e^{\pm 2i\theta}$ terms, whereas $[yz]$, $[zy]$, $[zx]$, and $[xz]$ contain only $e^{\pm i\theta}$ terms. So the LO deformation scattering is clearly ineffective in these configurations.

The LO scattering matrix element multiplied by either $[xy]$ or $[yx]$ gives, apart from noncontributing terms containing powers of $e^{i\theta}$, the following terms independent of θ:

$$D|P|^2(12N^3I_n)^{-1/2}[(\langle c|\Phi_n'|\bar{a}\rangle-\langle d|\Phi_n'|\bar{b}\rangle)\times((\bar{a}\,^*)(c)+(\bar{b}\,^*)(d))+(\langle a|\Phi_n'|\bar{c}\rangle-\langle b|\Phi_n'|\bar{d}\rangle)((\bar{c}\,^*)(a)+(\bar{d}\,^*)(b))]\delta_{E,\bar{E}}\ .$$

So that the products of the overlap integrals in the above expression do not vanish, the hole components appearing in the products must have the same parity. Therefore in carrying out the sum $\sum^{\pm}\overline{\sum}^{\pm}$, the terms arising from either reversing a,b,c,d or $\bar{a},\bar{b},\bar{c},\bar{d}$ alone make no contribution. As the expression remains unchanged on simultaneous reversal of both a,b,c,d and $\bar{a},\bar{b},\bar{c},\bar{d}$, so the sum $\sum^{\pm}\overline{\sum}^{\pm}$ just doubles the expression. Thus we get

$$\mathcal{N}_{SR}^{\mathrm{LO,DP}}(xy)=\mathcal{N}_{SR}^{\mathrm{LO,DP}}(yx)=D|P|^2(3N^3I_n)^{-1/2}[\,(\langle a|\Phi_n'|\bar{c}\rangle+\langle b|\Phi_n'|\bar{d}\rangle)\times((\bar{c}^{\,*})(a)+(\bar{d}^{\,*})(b))+(\langle c|\Phi_n'|\bar{a}\rangle+\langle d|\Phi_n'|\bar{b}\rangle)\times((\bar{a}^{\,*})(c)+(\bar{b}^{\,*})(d))]\delta_{E,\bar{E}}\ . \tag{40}$$

It will be useful to note that the TO1 and TO2 deformation-potential (DP) scattering matrix elements (17) and (18) are formally very similar. For deriving their SRN, the essential difference (i.e., granting that there is a trivial difference in the normalization constants and a change from Φ_n' to Ψ_n) is a change of sign of the $e^{-i\theta}$ terms.

As these scattering matrix elements contain only $e^{\pm i\theta}$ terms and $[xy]$ and $[yx]$ contain only $e^{\pm 2i\theta}$ terms or terms independent of θ, the TO1 and TO2 modes are clearly not active in these configurations.

The TO1 scattering matrix element multiplied by $[zx]$ gives the following terms not containing $e^{i\theta}$ factors:

$$iD|P|^2(3N^3I_n)^{-1/2}\left[\frac{\omega_{\mathrm{LO}}}{\omega_{\mathrm{TO}}}\right]^{1/2}[(\langle d|\Phi_n'|\bar{c}\rangle-\langle b|\Phi_n'|\bar{a}\rangle)((\bar{c}^{\,*})(d)+3^{-1/2}(\bar{b}^{\,*})(c))+(\langle a|\Phi_n'|\bar{b}\rangle-\langle c|\Phi_n'|\bar{d}\rangle)\times((\bar{b}^{\,*})(a)+3^{-1/2}(\bar{c}^{\,*})(b))]\delta_{E,\bar{E}}\ . \tag{41}$$

We note that (41) vanishes at it stands, as the hole components appearing in the products of overlap integrals are of opposite parities. However, in carrying out the $\sum^{\pm}\overline{\sum}^{\pm}$, nonvanishing terms arise from reversing either a,b,c,d or $\bar{a},\bar{b},\bar{c},\bar{d}$. In fact, it is found that the first term in the square brackets with a,b,c,d reversed equals the second term with $\bar{a},\bar{b},\bar{c},\bar{d}$ reversed, and the second term with a,b,c,d reversed equals the first term with $\bar{a},\bar{b},\bar{c},\bar{d}$ reversed. Therefore carrying out the sum $\sum^{\pm}\overline{\sum}^{\pm}$ is equivalent to (41) with either a,b,c,d or $\bar{a},\bar{b},\bar{c},\bar{d}$ reversed, then multiplied by 2. Thus we get

$$\mathcal{N}_{SR}^{\mathrm{TO1,DP}}(xz)=i2D|P|^2(3N^3I_n)^{-1/2}\left[\frac{\omega_{\mathrm{LO}}}{\omega_{\mathrm{TO}}}\right]^{1/2}\times[(\langle a|\Phi_n'|\bar{c}\rangle-\langle c|\Phi_n'|\bar{a}\rangle)\times((\bar{c}^{\,*})(a)+3^{-1/2}(\bar{b}^{\,*})(b))+(\langle d|\Phi_n'|\bar{b}\rangle-\langle b|\Phi_n'|\bar{d}\rangle)((\bar{b}^{\,*})(d)+3^{-1/2}(\bar{c}^{\,*})(c))]\delta_{E,\bar{E}}\ . \tag{42}$$

If we change over to TO2, we find that owing to the above-mentioned sign difference in the $e^{-i\theta}$ terms in its scattering matrix element as compared to TO1, its formula corresponding to (41) would have a negative sign in front of the first term in the square brackets. It is readily seen that owing to such a difference, the terms arising from reversing a,b,c,d will exactly cancel rather than equal the terms arising from reversing $\bar{a},\bar{b},\bar{c},\bar{d}$. In other words, terms arising from the sum $\sum^{\pm}\overline{\sum}^{\pm}$ exactly cancel out; thus TO2 will not be active in this configuration.

With the case of TO1 scattering matrix elements multiplied by $[xz]$, the situation with the summation process is exactly analogous to the above case. The result is

$$\mathcal{N}_{SR}^{\mathrm{TO1,DP}}(zx)=-i2D|P|^2(3N^3I_n)^{-1/2}\left[\frac{\omega_{\mathrm{LO}}}{\omega_{\mathrm{TO}}}\right]^{1/2}\times[(\langle a|\Phi_n'|\bar{c}\rangle-\langle c|\Phi_n'|\bar{a}\rangle)\times((\bar{a}^{\,*})(c)+3^{-1/2}(\bar{b}^{\,*})(b))+(\langle d|\Phi_n'|\bar{b}\rangle-\langle b|\Phi_n'|\bar{d}\rangle)((\bar{d}^{\,*})(b)+3^{-1/2}(\bar{c}^{\,*})(c))]\delta_{E,\bar{E}}\ . \tag{43}$$

Similar to the above (xz) case, the TO2 mode is not active in this configuration.

Working out the TO2 case with (zy) and (yz) closely parallels the case of TO1 with (zx) and (xz). The following results are obtained:

$$\mathcal{N}_{SR}^{\mathrm{TO2,DP}}(yz)=2D|P|^2(3N^3)^{-1/2}\left[\frac{2d\omega_{\mathrm{LO}}}{w\omega_{\mathrm{TO}}}\right]^{1/2}\times[(\langle a|\Psi_n|\bar{c}\rangle-\langle c|\Psi_n|\bar{a}\rangle)\times((\bar{b}^{\,*})(d)+3^{-1/2}(\bar{c}^{\,*})(c))+(\langle d|\Psi_n|\bar{b}\rangle-\langle b|\Psi_n|\bar{d}\rangle)((\bar{c}^{\,*})(a)+3^{-1/2}(\bar{b}^{\,*})(b))]\delta_{E,\bar{E}}\ , \tag{44}$$

$$\mathcal{N}_{SR}^{\mathrm{TO2,DP}}(zy)=2D|P|^2(3N^3)^{-1/2}\left[\frac{2d\omega_{\mathrm{LO}}}{w\omega_{\mathrm{TO}}}\right]^{1/2}\times[(\langle a|\Psi_n|\bar{c}\rangle-\langle c|\Psi_n|\bar{a}\rangle)\times((\bar{a}^{\,*})(c)+3^{-1/2}(\bar{b}^{\,*})(b))+(\langle d|\Psi_n|\bar{b}\rangle-\langle b|\Psi_n|\bar{d}\rangle)((\bar{d}^{\,*})(b)+3^{-1/2}(\bar{c}^{\,*})(c))]\delta_{E,\bar{E}}\ . \tag{45}$$

TABLE II. The allowed Raman scatterings for various phonon modes, scattering mechanisms, and polarization schemes.

Polarization	Phonon and parity	Interaction	Formula
(xx)	LO even $\Phi_n(z)$	F	(31)
(yy)	LO even $\Phi_n(z)$	F	(32)
(zz)	LO even $\Phi_n(z)$	F	(33)
(xy)	LO odd $\Phi_n(z)$	DP	(40)
(yx)	LO odd $\Phi_n(z)$	DP	(40)
(xz)	TO1 odd $\Phi_n(z)$	DP	(42)
(zx)	TO1 odd $\Phi_n(z)$	DP	(43)
(yz)	TO2 even $\Psi_n(z)$	DP	(44)
(zy)	TO2 even $\Psi_n(z)$	DP	(45)

When we change over to TO1 with $[zy]$ and $[yz]$, we find that owing to the sign difference originating in the $e^{-i\theta}$ terms in the scattering matrix element, the summation leads to terms that exactly cancel.

As explained earlier, the calculated SRN should show the symmetry features of the Raman tensor. Table II is a summary of such symmetry features shown by the SRN derived above. The table lists the phonon modes and scattering mechanisms active in various polarization configurations. The phonon parities for the depolarized configurations are derived from the fact that the interaction matrix elements are matrix elements of Φ_n' and Ψ_n between hole components of the same parity.

Practically all the experimental works on Raman scattering in MQW's reported in the literature are carried out essentially in the backscattering configuration, so the only polarization configurations feasible are (xx), (yy), (xy), and (yx). From Table II, we see that only the LO modes are observable. So the experimental results on 90° scattering reported by Zucker *et al.* are of particular interest.[19] In this case, the possible polarization configurations include (xx), (zx), (xy), and (zy). In Fig. 1 the observed Raman spectra for all these configurations are reproduced. The observed peaks are seen to agree with those expected from Table II (not as claimed by Zucker *et al.*, that just the bulk deformation potential could not account for their experiments). The TO peaks observed in (zx) and (zy) configurations should represent the two different types of TO modes, and the LO modes observed in (xx) and (xy) configurations should separately represent even and odd LO modes. Such differences are, however, not well resolved.

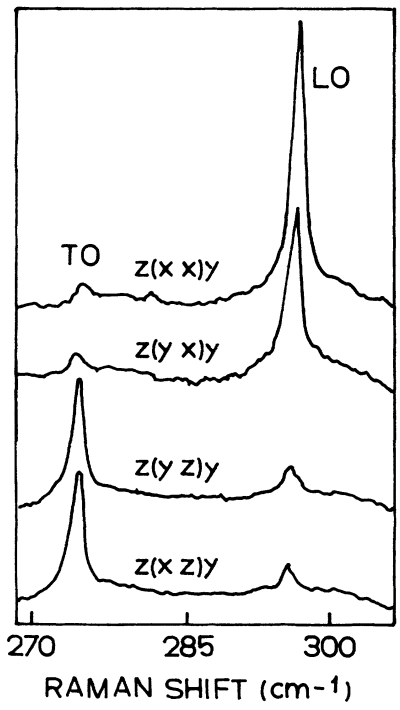

FIG. 1. Right-angle Raman spectra by Zucker *et al.* (Ref. 13).

VI. SPECIAL DISCUSSION ON FRÖHLICH SCATTERING

Raman scattering due to Fröhlich interaction in MQW's is of particular interest. As in the case of bulk materials, in the dipole approximation, Fröhlich interaction is not effective in Raman scattering. The results deduced above show apparently that even in the dipole approximation Fröhlich interaction does contribute to the Raman scattering in MQW's. However, this point warrants closer examination. As we shall see, nonvanishing contribution by Fröhlich interaction, in fact, depends intricately on certain features of hole and electron wave functions in quantum wells.

Thus if we ignore heavy- and light-hole mixing, the hole wave function will reduce to its major component. If, moreover, barrier-penetration effects are neglected, the major hole component as well as the electron wave function will both be associated with standing wave functions along the z axis; between them, orthogonality with respect to the subband quantum number n holds. In such a case, as Δn must be zero for both intermediate electron-hole pairs [in virtue of electron-hole overlap integrals in (39)], the electron and hole subband quantum numbers n must remain unchanged in the scattering. Besides, for nonvanishing Fröhlich scattering of holes, the major hole components of the two intermediate states must be matched [see Eq. (39)]. It follows from these requirements that the Fröhlich scattering of either the electron or hole can be effective only within the same subband (i.e., only in intrasubband scattering).

But with the neglect of heavy- and light-hole mixing and barrier-penetration effects, the hole scattering factor

$$\langle a|V|a\rangle+\langle b|V|b\rangle+\langle c|V|c\rangle+\langle d|V|d\rangle$$

reduces to a single diagonal matrix element formed from the major hole component, which is just the same standing wave function as the electron function. Therefore, comparing (39) and (40), we see that even in the case of intrasubband scattering the contributions from electron and hole scattering cancel, leading to a zero result.

Thus, we see that finite contributions by Fröhlich interaction must ultimately be derived from such intricate features of the hole and electron wave functions as heavy- and light-hole mixing and barrier penetration. In the following, we shall look into the problem in more detail by some model calculations of the symmetrized Raman

numerator as given in (31) and (32) for LO Fröhlich scattering by the lowest-order mode ($n=2$ mode).

In Figs. 2 and 3 are shown the calculated SRN's as a function of $k_{\parallel}$ for intersubband and intrasubband scattering between HH1-CB1, LH1-CB1, and HH2-CB1; in other words, for scattering between electron-hole pairs formed from electrons in its first subband (CB1) and holes in either of the three lowest hole subbands, namely, the first heavy-hole band (HH1), first light-hole band (LH1), and second heavy-hole band (HH2). They are calculated with the infinite-barrier model for the quantum well, so that barrier-penetration effects are excluded and we can examine the heavy- and light-hole mixing effects alone.

Consider first the intersubband scattering cases illustrated in Fig. 2. Since at $k_{\parallel}=0$, the hole wave function reduces to its major component, at this limit there is no heavy- and light-hole mixing and Fröhlich scattering is expected to lead to a zero result. We see, in fact, that in all three cases illustrated the curves tend to zero as $k_{\parallel}\rightarrow 0$.

The detailed structures are seen, however, to be very different in the three cases, indicating their sensitivity to specific features of heavy- and light-hole mixing and hole subband structures. Two marked features in the figure especially merit some comments.

We note that the LH1-CB1 and HH2-CB1 case shows a particularly steep rise in magnitude with $k_{\parallel}$, as $k_{\parallel}$ increases from zero, so that even at very small $k_{\parallel}$ values it has already reached a considerable magnitude. This reflects a well-known feature of hole subbands for a quantum well of GaAs, namely, near $k_{\parallel}=0$, there is strong interaction and intermixing between the LH1 and HH2. This interaction is clearly evidenced in the negative curvature of the LH1 subband at $k_{\parallel}=0$ seen in the hole subband dispersion curves illustrated in Fig. 4.

Another marked feature is the practically discontinuous structures observed in the cases of LH1-CB1 to HH2-CB1 and HH1-CB1 to HH2-CB1. By comparing this with the hole subband dispersion curves, we see that

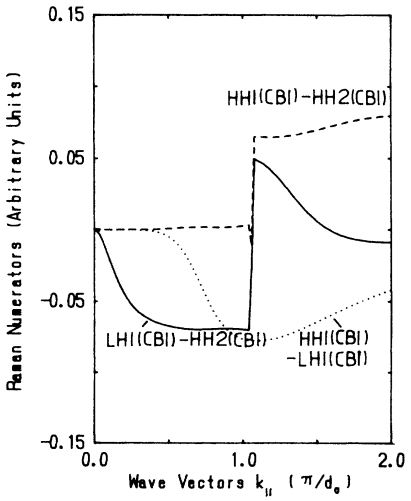

FIG. 2. Symmetrized Raman numerator for intersubband Fröhlich scattering calculated with an infinite-barrier model.

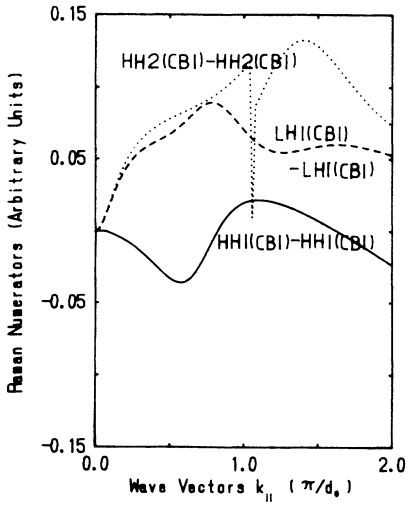

FIG. 3. Symmetrized Raman numerator for intrasubband Fröhlich scattering calculated with an infinite-barrier model.

this clearly has its origin in the sharp change of HH2 at the point where HH2 and HH3 dispersion curves effectively cross over. In other words, to the right of the abrupt jumps observed in Fig. 2, HH2 is effectively replaced by HH3, which has a major component matched with HH1 (both having d as the major component).

We note that the same hole mixing features are observable in the intrasubband scattering cases in Fig. 3, namely, the rapid rise near $k_{\parallel}=0$ in the cases of LH1-CB1 and HH2-CB1 due to their mixing, and the abrupt change associated with the HH2 and HH3 interaction. In this case, a further noteworthy feature is the considerable magnitude of the intrasubband scattering with HH2-CB1, even though it is a case of $\Delta n\neq 0$. First, this means that hole mixing effects can effectively promote otherwise forbidden scattering involving $\Delta n\neq 0$ pairs. Second, $\Delta n\neq 0$ intrasubband scattering has, in fact, an advantage over

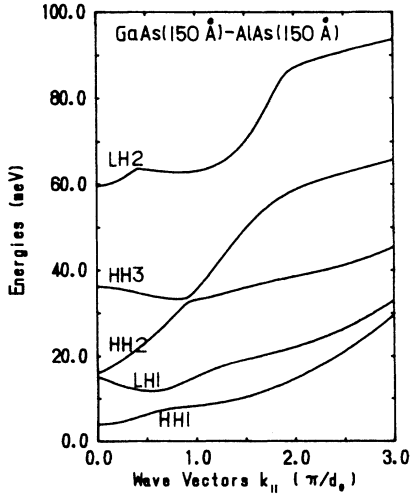

FIG. 4. Hole subband dispersion curves for GaAs(150 Å)/AlAs(150 Å) MQW's.

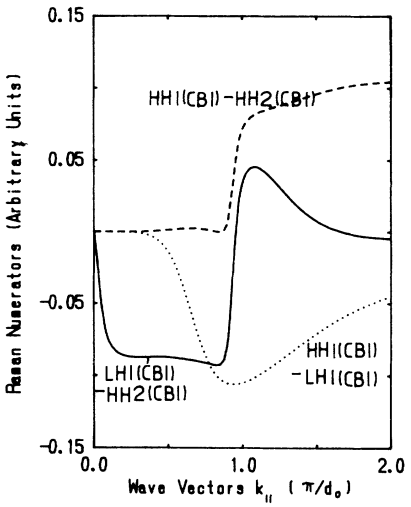

FIG. 5. Symmetrized Raman numerator for intersubband Fröhlich scattering in GaAs(150 Å)/AlAs(150 Å) MQW's calculated with a finite-barrier model.

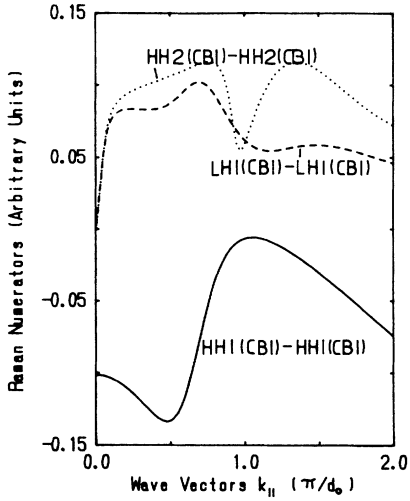

FIG. 6. Symmetrized Raman numerator for intrasubband Fröhlich scattering in GaAs(150 Å)/AlAs(150 Å) MQW's calculated with a finite-barrier model.

$\Delta n = 0$ cases in the greater dissimilarity between electron and hole wave functions. Apparently this reduces the cancellation between the electron and hole scattering effects so effectively that the HH2-CB1 pair exhibits stronger intrasubband scattering than the other two instances (involving $\Delta n = 0$ pairs).

Figure 5 gives the SRN for intersubband Fröhlich scatterings similar to that in Fig. 2, but calculated with a finite-barrier model (with parameters simulating GaAs-AlAs MQW's) with a well width of 150 Å. They are seen to be fairly closely similar to the results calculated with the infinite-barrier model. This shows that the intersubband scatterings are predominantly determined by hole mixing effects; barrier penetration plays only a very minor role.

Barrier penetration can, however, be important in intrasubband scattering. Thus in the intrasubband scattering results calculated with the finite-barrier model, as illustrated in Fig. 6, one sees that the HH1-CB1 result is very different from the corresponding result in Fig. 3. The difference is seen to be not so much a change of shape of the curve, but rather a vertical shift of the curve. This is what is to be expected, as the important effect of barrier penetration is a change in the net charge (electron plus hole) enclosed in the well region, which alone is effective in interacting with the strictly confined LO mode.

VII. SCATTERING BY INTERFACE MODES

According to the dielectric continuum model, in a superlattice there are, besides the confined bulklike modes discussed in Sec. III, also a number of so-called interface modes.[12] We have shown that, unlike the bulklike modes, these modes are unambiguously determined by the continuum model and agree completely with results calculated from a parallel microscopic model (also neglecting phonon dispersion).[18] For the sake of simplicity, in the following we shall discuss scattering by the interface modes, quoting needed results from the continuum model without proof. Moreover, we shall suppose the superlattice to have layers of equal thickness d_0 for the two materials, with d_0 related to the superlattice period d by $d = 2d_0$. With superlattices like the GaAs-AlAs system in mind, we shall suppose the ω_{LO}-ω_{TO} gaps of the two materials to be nonoverlapping.

For such a model, for a given wave vector $\mathbf{k}$, there are four interface modes with frequencies given implicitly by the following equation:

$$\cos(k_z d) = \frac{\epsilon^2+\bar{\epsilon}^2}{2\epsilon\bar{\epsilon}}\sinh(k_{\parallel}d_0)\sinh[k_{\parallel}(d-d_0)] + \cosh(k_{\parallel}d_0)\cosh[k_{\parallel}(d-d_0)] \, . \tag{46}$$

Letters with or without an overbar are used to label physical quantities for the two materials. Thus $\epsilon, \bar{\epsilon}$ are the dielectric functions of the two materials:

$$\epsilon(\omega) = \epsilon_\infty \frac{\omega_{\mathrm{LO}}^2-\omega^2}{\omega_{\mathrm{TO}}^2-\omega^2}, \quad \bar{\epsilon}(\omega) = \bar{\epsilon}_\infty \frac{\bar{\omega}_{\mathrm{LO}}^2-\omega^2}{\bar{\omega}_{\mathrm{TO}}^2-\omega^2} \, .$$

In the LO-TO gap of each material fall two of the solutions, which approach separately the LO and TO frequencies as $\mathbf{k}$ approaches the z axis (i.e., $k_{\parallel} \to 0$).

The optical displacement of the interface modes can be generally expressed in terms of their normal coordinates as follows:

$$\mathbf{u}(\mathbf{r})=(8MN^3)^{-1/2}[1-\cos(k_z d)]^{-1/2}[(\bar{\epsilon}-\epsilon)(\bar{\epsilon}S^2-\epsilon\bar{S}^2)]^{-1/2}[k_\parallel d_0/\sinh(k_\parallel d)]^{1/2}$$
$$\times\sum_l\left[S(\omega)\begin{pmatrix}0\\ i(Ae^{k_\parallel z_l}-Be^{-k_\parallel z_l})\\ -(Ae^{k_\parallel z_l}+Be^{k_\parallel z_l})\end{pmatrix}_{z_l=z-ld}\right.$$
$$\left.+\bar{S}(\omega)\begin{pmatrix}0\\ i(\bar{A}e^{k_\parallel \bar{z}_l}-\bar{B}e^{-k_\parallel \bar{z}_l})\\ -(\bar{A}e^{k_\parallel \bar{z}_l}+\bar{B}e^{-k_\parallel \bar{z}_l})\end{pmatrix}_{\bar{z}_l=z-ld-d_0}\right]e^{-ik_\parallel y-ik_z ld}Q(\mathbf{k},m)\ , \tag{47}$$

where $m=1,2,3,4$ labels the four solutions of (46). For brevity, we have introduced the following notation:

$$S(\omega)=\epsilon_\infty^{1/2}\frac{(\omega_{\rm LO}^2-\omega_{\rm TO}^2)^{1/2}}{\omega_{\rm TO}^2-\omega^2},\quad \bar{S}(\omega)=\bar{\epsilon}_\infty^{1/2}\frac{(\bar{\omega}_{\rm LO}^2-\bar{\omega}_{\rm TO}^2)^{1/2}}{\bar{\omega}_{\rm TO}^2-\omega^2}\ .$$

We note that z_l and $\bar{z}_l$ are used to represent the z coordinates within the lth layer of the two materials; therefore the exponential functions should be considered as only defined with $|z_l|<d_0/2$ and $|\bar{z}_l|<d_0/2$. The coefficients $A,B,\bar{A},\bar{B}$ are given by

$$A=(\bar{\epsilon}-\epsilon)\exp(-0.5k_\parallel d_0)+(\bar{\epsilon}+\epsilon)\exp(1.5k_\parallel d_0)-2\bar{\epsilon}\exp(-0.5k_\parallel d_0)\exp(ik_z d)\ ,$$
$$B=(\bar{\epsilon}-\epsilon)\exp(0.5k_\parallel d_0)+(\bar{\epsilon}+\epsilon)\exp(-1.5k_\parallel d_0)-2\bar{\epsilon}\exp(0.5k_\parallel d_0)\exp(ik_z d)\ ,$$
$$\bar{A}=(\bar{\epsilon}-\epsilon)\exp(0.5k_\parallel d_0)-(\bar{\epsilon}+\epsilon)\exp(-1.5k_\parallel d_0)+2\epsilon\exp(0.5k_\parallel d_0)\exp(-ik_z d)\ ,$$
$$\bar{B}=(\bar{\epsilon}-\epsilon)\exp(-0.5k_\parallel d_0)-(\bar{\epsilon}+\epsilon)\exp(1.5k_\parallel d_0)+2\epsilon\exp(-0.5k_\parallel d_0)\exp(-ik_z d)\ .$$

The electrostatic potential associated with the mode is given by

$$V(\mathbf{r})=[\pi/(2N^3v_0)]^{1/2}[1-\cos(k_z d)]^{1/2}[(\bar{\epsilon}-\epsilon)(\bar{\epsilon}S^2-\epsilon\bar{S}^2)]^{-1/2}[k_\parallel d_0/\sinh(k_\parallel d)]^{1/2}$$
$$\times k_\parallel^{-1}\sum_{l,m}[(Ae^{k_\parallel z_l}-Be^{-k_\parallel z_l})+(\bar{A}e^{k_\parallel \bar{z}_l}-\bar{B}e^{-k_\parallel \bar{z}_l})]e^{-ik_\parallel y-ik_z ld}Q(\mathbf{k},m)\ . \tag{48}$$

As we shall be interested in modes with very small kd, we shall express $V(\mathbf{r})$ as series expansion in $k_\parallel d_0$, $k_\parallel z_l$, $k_\parallel \bar{z}_l$, and $k_z d$, and concentrate on the lowest-order terms that give nonvanishing scattering. The lowest-order terms in the expansion of $V(\mathbf{r})$ turn out to be to the power -1 of k, namely,

$$V_{-1}(\mathbf{r})=(2\pi N^{-3}v_0^{-1})^{1/2}(\epsilon+\bar{\epsilon})[(\bar{\epsilon}-\epsilon)(\bar{\epsilon}S^2-\epsilon\bar{S}^2)]^{-1/2}k_z^{-1}e^{-ik_\parallel y-ik_z ld}Q(\mathbf{k},m)\ , \tag{49}$$

in the lth period, where the suffix -1 attached to $V(\mathbf{r})$ expresses that only terms of the order k^{-1} are included. Equation (49) tells us that the lowest-order terms represent a constant scattering potential within a period of the superlattice. Thus neither electron nor hole intersubband scattering would be possible, owing to the orthogonality between wave functions from different subbands (for the same k). On the other hand, for intrasubband scattering, the scattering intergals for holes and electrons reduce simply to $\pm e$ multiplied by the same constant potential and hence exactly cancel, leading to a zero result. In other words, to this order Fröhlich interaction is ineffective.

The next-higher-order terms correspond to zeroth power of k, namely,

$$V_0(\mathbf{r})=id(2\pi N^{-3}v_0^{-1})^{1/2}[(\bar{\epsilon}-\epsilon)(\bar{\epsilon}S^2-\epsilon\bar{S}^2)]^{-1/2}$$
$$\times\sum_l\left[\left[\frac{\bar{\epsilon}}{2}-\bar{\epsilon}\frac{z_l}{d_0}\right]_{z_l=z-ld}-\left[\frac{\epsilon}{2}+\epsilon\frac{\bar{z}_l}{d_0}\right]_{\bar{z}_l=z-ld-d_0}\right]e^{-ik_\parallel y-ik_z ld}Q(\mathbf{k},m)\ . \tag{50}$$

As we have seen in Sec. V, for nonvanishing Fröhlich scattering, the interaction potential must be even in z in the quantum well. Therefore only the constant parts in the expression can be active in Raman scattering. We note that the essential difference of the constant potentials in (50) from the previous V_{-1} potential is that now the constant potentials in the two materials are different. However, if we neglect the penetration of the carriers into the barriers so that the carriers are strictly confined in one material, they would see only a constant potential and hence could not induce scattering just as in the case of V_{-1}. Thus, to this order, scattering occurs solely in virtue of the partial penetration of the carrier wave functions into the barrier regions.

For the consideration of deformation-potential scattering, we express the optical displacement (47) as a power series in k. We find that the lowest-order terms in this case correspond to the zeroth power of k, namely,

$$\mathbf{u}_0(\mathbf{r})=(2MN^3)^{-1/2}[(\bar{\epsilon}-\epsilon)(\bar{\epsilon}S^2-\epsilon\bar{S}^2)]^{-1/2}$$

$$\times\sum_l\left[S(\omega)\begin{bmatrix}0\\ i\frac{k_\parallel}{k_z}(\epsilon+\bar{\epsilon})\\ i2\bar{\epsilon}\end{bmatrix}_{z_l}+\bar{S}(\omega)\begin{bmatrix}0\\ i\frac{k_\parallel}{k_z}(\epsilon+\bar{\epsilon})\\ i2\epsilon\end{bmatrix}_{\bar{z}_l}\right]e^{-ik_\parallel y-ik_z ld}Q(\mathbf{k},m)\ . \tag{51}$$

Using the deformation potentials (11) and (12), the hole scattering matrix element can be written down exactly analogously to the derivation of (15) and (17) for the bulklike modes. Thus we get

$$\langle\bar{H}^+|H_{EL}|H^+\rangle=D(2N^3)^{-1/2}\left[\frac{\omega_{\rm LO}}{\omega}\right]^{1/2}S[(\bar{\epsilon}-\epsilon)(\bar{\epsilon}S^2-\epsilon\bar{S}^2)]^{-1/2}$$

$$\times\{2\bar{\epsilon}[e^{2i\theta}(\langle a|\bar{c}\rangle+\langle b|\bar{d}\rangle)-e^{-2i\theta}(\langle c|\bar{a}\rangle+\langle d|\bar{b}\rangle)]$$

$$-[k_\parallel(\epsilon+\bar{\epsilon})/k_z][e^{i\theta}(\langle a|\bar{b}\rangle-\langle c|\bar{d}\rangle)-e^{-i\theta}(\langle b|\bar{a}\rangle-\langle d|\bar{c}\rangle)]\}\ , \tag{52}$$

where we have taken the quantum well as located in the material designated by letters without an overbar.

Since in the case of wave vector $\mathbf{k}$ parallel to the z axis the interface modes are no longer distinct from the bulk frequencies, the usual backscattering configuration would not be suitable for investigation of interface-mode scattering. Explicitly, we shall consider 90° scattering, which will be the y direction by our convention and the phonon vector will be along a 45° direction with $k_\parallel=k_z$. For such 90° scattering, only the polarization configurations (xx), (xz), (yx), and (yz) need be considered. We can work out the $\mathcal{N}_{SR}(ij)$ for these polarization configurations according to (26) with the help of (ij) given in Sec. V exactly in the manner of the bulklike modes. We shall not go into details. It is found that the interface modes give nonvanishing scattering only in the polarization configurations $[xz]$ and $[yx]$; for these two cases the SRN's are found to be given by

$$\mathcal{N}_{SR}^{\rm IF,DP}(xz)=-i2D|P|^2(6N^3)^{-1/2}\left[\frac{\omega_{\rm LO}}{\omega}\right]^{1/2}S(\epsilon+\bar{\epsilon})[(\bar{\epsilon}-\epsilon)(\bar{\epsilon}S^2-\epsilon\bar{S}^2)]^{-1/2}$$

$$\times[(\langle a|\bar{c}\rangle-\langle c|\bar{a}\rangle)((\bar{c}^*)(a)+3^{-1/2}(\bar{b}^*)(b))+(\langle d|\bar{b}\rangle-\langle b|\bar{d}\rangle)((\bar{b}^*)(d)+3^{-1/2}(\bar{c}^*)(c))]\delta_{E,\bar{E}}\ .$$

$$\mathcal{N}_{SR}^{\rm IF,DP}(yx)=i2D|P|^2(6N^3)^{-1/2}\left[\frac{\omega_{\rm LO}}{\omega}\right]^{1/2}S\bar{\epsilon}[(\bar{\epsilon}-\epsilon)(\bar{\epsilon}S^2-\epsilon\bar{S}^2)]^{-1/2}$$

$$\times[(\langle a|\bar{c}\rangle+\langle b|\bar{d}\rangle)((\bar{c}^*)(a)+(\bar{d}^*)(b))+(\langle d|\bar{b}\rangle+\langle c|\bar{a}\rangle)((\bar{b}^*)(d)+(\bar{a}^*)(c))]\delta_{E,\bar{E}}\ .$$

It is easily verified that these SRN's should be comparable to those pertaining to the bulklike modes in magnitude. however, it is very regretable that the only results on 90° scattering given by Zucker *et al.*,[19] as already cited in Fig. 1, cannot provide positive evidence for scattering by interface modes. The GaAs(96 Å)/$Ga_{0.72}Al_{0.29}As$(98 Å) superlattice specimens have their GaAs-like modes so close in frequency to the modes of the GaAs layers, one can hardly expect the peaks due to the interface modes to be clearly resolved from the bulklike modes.

VIII. COMMENTS ON EXCITON-MEDIATED SCATTERING

To be accurate, one should, of course, take into account the Coulomb interaction between the electron-hole pairs. The most important consequence is that the electron-hole pair can be bound to form discrete exciton states, which are basic to the consideration of resonant Raman scattering. A theoretical treatment of Raman scattering based on discrete exciton states as intermediate states has been recently published by the present authors in a separate paper.[26] In the following, we shall just comment on certain main features of exciton mediated scattering.

The basic feature to be emphasized is the complex angular momentum structure of the quasi-2D excitons in quantum wells.[23,24] Namely, the four hole components of the exciton wave function are associated with different orbital angular momenta in the x-y plane representable as $\hbar(j-j_0)$, where j labels the different hole components. j_0 serves as a parameter specifying the angular momentum of the exciton as a whole; once j_0 is given, the angular momentum associated with each hole component is specified. j_0 itself has a simple meaning, it is just the label for the component with zero angular momentum.

The angular momenta of the intermediate discrete excitons play a decisive role in all three matrix elements in the Raman numerator.

(1) The two photon interaction matrix elements are just the optical transition matrix elements relating to usual exciton absorption and emission processes. It can be readily proven that only the j_0 component of the exciton wave function contributes to these matrix elements.

In the theoretical treatment of quasi-two-dimensional

(2D) excitons in quantum wells, we have found it convenient to introduce conventional orbital angular momentum designation to specify 2D excitons, namely, we specify an exciton as in $s,p,d,\ldots$ states in the conventional way according to the angular momentum associated with its dominant hole component. Thus it follows that, from the point of view of the photon interaction matrix elements, α and β should be s-state excitons to give the largest SRN. In other words, important resonances are expected to be associated with s-state excitons.

(2) The angular momenta of the α and β excitons also play a decisive role in the phonon-scattering matrix element. With Fröhlich interaction, the scattering is nonvanishing only when j_0 for α exciton and j_0' for β exciton are equal. In other words, the angular momenta of the corresponding hole components of the two excitons must be completely matched. This is related to the fact that the Fröhlich interaction potential is slowly varying and the integration over the band-edge functions results in orthogonality factors which couple together only the corresponding hole components of the two excitons.

That j_0 must equal j_0', coupled with the requirement that both excitons should be s-state excitons, implies that excitons important to resonance scattering should be formed from hole subbands with similar dominant hole components.

In contrast to Fröhlich scattering, we see readily from Eqs. (10)–(12) that the deformation-potential interaction couples together hole components of the two excitons, which are relatively shifted by one (for x and y displacements) or two (for z displacements) places. From this it follows that for nonvanishing scattering, the angular momenta associated with the hole components of the two excitons must be subject to such "shifted matching." In other words, for deformation-potential scattering by LO modes (z displacements) we must have $j_0'=j_0\pm2$ and for scattering by TO1 and TO2 modes, we must have $j_0'=j_0\pm1$. Now if α and β are both s-state excitons for strong resonance, the above requirements mean that their dominant components should be relatively shifted by one or two places. This circumstance implies that the two excitons must separately be heavy- light-hole excitons.

Calculations of SRN have been carried out for various possible exciton pairs in a number of superlattice structures. Table III gives the results calculated for Fröhlich scattering by the LO mode in a GaAs(102 Å)/$Al_{0.27}Ga_{0.73}As$(207 Å) superlattice. Listed in Table III are the 10 cases, which give the largest SRN.

The results are seen to verify that in most cases these strongest resonances are associated with s-state excitons. Cases 1, 7, and 10 appear to violate this rule, as they involve $2p$ excitons. This actually expresses an effect of extra strong heavy- and light-hole mixing. As we have emphasized earlier, even for very small $k_{\parallel}$, LH1 and HH2 subbands are strongly intermixed. We note that the second hole component b is the dominant component of LH1 holes, and the first hole component a is the dominant component of HH2 holes. As the listed LH1 $2p$ has its first component with s angular momentum, intermixing of HH2 has the effect of greatly strengthening this component; the net results make the LH1 $2p$ acquire the typical character of HH2 $1s$ (i.e., strong first component with zero angular momentum). With this understanding, the apparent anomaly of cases 1, 7, and 10 is naturally explained.

According to the above discussions about Fröhlich interaction, the dominant components of the α and β excitons should be mutually matched . As HH1 and HH3 both have their fourth components d as their dominant components, and HH2 and HH4 have their first components a as their dominant components, we see from the above table that the dominant components of α and β excitons do match in all cases, except cases 7 and 10. But as we have explained the excitons listed in LH1 $2p$ in cases 7 and 10 apparently assume to a large measure the typical character of HH2 $1s$. Regarded in this light, we might consider these two cases as also fulfilling the above matching condition.

Table IV gives similar results calculated for deformation-potential scattering by the LO mode (both tables deal with the lowest-order modes of the required symmetry). In the table are again listed 10 cases which give the largest SRN. The tabulated results verify that all cases except nos. 3, 4, and 10 are derived from intersubband scattering of s-state excitons between heavy- and light-hole subbands. The apparent deviation of cases 3, 4, and 10 from this rule is readily understood in terms of the strong intermixing between the LH1 and HH2 subbands. Apparently, owing to this mixing, the listed LH1 $2p$ in cases 3 and 10 assumes very much the character of HH2

TABLE III. The ten Fröhlich scattering channels (via first $A1$ phonon mode) for the 102-Å-wide sample, which gives the largest SRN.

Case no.	α	β	SRN
1	LH1-CB2 $2p$	LH1-CB2 $2p$	−169.6
2	HH1-CB1 $1s$	HH3-CB1 $1s$	138.6
3	HH1-CB1 $1s$	HH1-CB1 $1s$	−118.9
4	HH3-CB3 $1s$	HH3-CB3 $1s$	−96.5
5	HH2-CB2 $1s$	HH2-CB2 $1s$	−90.4
6	HH2-CB2 $1s$	HH4-CB2 $1s$	64.8
7	LH1-CB2 $2p$	HH4-CB2 $1s$	39.8
8	HH3-CB1 $1s$	HH3-CB1 $1s$	39.8
9	HH3-CB1 $1s$	HH3-CB1 $1s$	−37.9
10	LH1-CB2 $2p$	HH2-CB2 $1s$	33.3

TABLE IV. The ten scattering channels through deformation-potential interaction (via first $B2$ phonon mode) for the 102-Å-wide sample, which gives the largest SRN.

Case no.	α	β	SRN
1	HH1-CB1 $1s$	LH1-CB1 $1s$	−75.28
2	HH2-CB2 $1s$	LH2-CB2 $1s$	−22.95
3	LH1-CB2 $2p$	LH2-CB2 $1s$	−11.8
4	HH1-CB1 $1s$	HH2-CB1 $2p$	−7.486
5	HH1-CB1 $2s$	LH1-CB1 $2s$	−7.395
6	HH2-CB2 $2s$	LH2-CB2 $2s$	−3.998
7	LH2-CB2 $1s$	HH4-CB2 $1s$	3.937
8	HH3-CB2 $1s$	LH3-CB2 $1s$	−3.311
9	HH1-CB1 $1s$	LH1-CB1 $2s$	3.275
10	LH1-CB2 $2p$	LH2-CB2 $2s$	−3.038

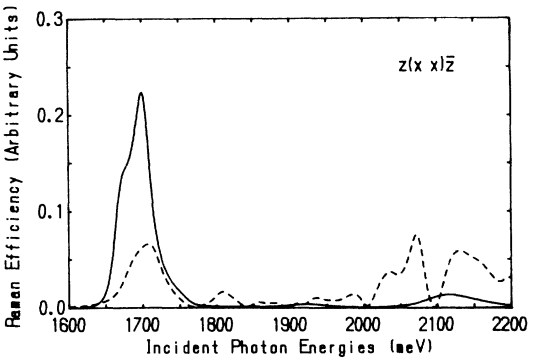

FIG. 7. Calculated squared xx component of the Raman tensor for the GaAs(50 Å)/AlAs(150 Å) MQW's associated with the $n=2$ phonon mode vs the incident energies. The intermediate states are discrete excitons (solid line) and electron-hole pairs (dashed line).

$1s$ and the HH2 $2p$ assumes much of the character of LH1 $1s$.

As an example, we calculated the resonant Raman profile for GaAs(50 Å)/AlAs(150 Å) MQW's in the $z(xx)\bar{z}$ configuration. We have taken both the free electron-hole pair and discrete exciton states to be intermediate states. The intermediate exciton states are calculated by using the variational method of Ref. 23. As shown in Fig. 7, the most obvious resonant peak is contributed by the HH1-CB1 $1s$ excitons, while some peaky structures at higher incident energies are derived from the electron-hole pair. One interesting point is that while the exciton-related peaks are located at energies of either excitonic transition or that with one phonon energy higher, the peaks derived from the electron-hole pair are not always at the subband edges, the reason being simply that near $k_{\parallel}=0$ intersubband Fröhlich scattering tends to zero. In calculating the resonant profile we have included all the confined subbands and used a damping factor to simulate inhomogeneity effects.

IX. CONCLUSIONS

Microscopic theory for optic-phonon Raman scattering in MQW's has been worked out systematically both for free electron-hole pairs and for discrete exciton states as intermediate states. The contributions by the electron-hole pairs show strong characteristic dependence on their parallel wave vector $k_{\parallel}$. They are closely related to the subband structures of the quantum wells, in which heavy- and light-hole mixing plays an important role. Exciton mediated scattering bears a close relation to electron-hole pair contributions of small $k_{\parallel}$, e.g., with respect to relative contributions from different subbands, and to variations with quantum-well parameters, etc. However, a distinguishing feature of exciton-mediated scattering is the decisive role of the angular momentum state of the intermediate excitons; namely, s-state excitons predominate in the scattering.

Scattering through Fröhlich interaction is no longer dipole forbidden in MQW's. As this marks an important difference from bulk materials scattering, more space has been given to the discussion of this type of scattering, showing that it depends ultimately on barrier penetration and hole-mixing effects. Owing to this difference from bulk materials, the special role of Fröhlich scattering close to exciton resonance scattering in bulk materials is absent in MQW's.

ACKNOWLEDGMENTS

This work was supported by the Chinese National Natural Science Foundation.

[1]M. V. Klein, IEEE J. Quantum Electron. **QE-22**, 1760 (1986).
[2]M. Cardona, Superlatt. Microstruct. **5**, 27 (1989).
[3]B. Jusserand and M. Cardona, in *Light Scattering in Solids V*, edited by M. Cardona and G. Güntherodt (Springer, Berlin, 1989), and references therein.
[4]J. Menéndez, J. Lumin (to be published).
[5]C. Colvard, R. Merlin, M. V. Klein, and A. C. Gossard, Phys. Rev. Lett. **43**, 298 (1980).
[6]B. Jusserand, D. Paquet, and A. Regreny, Phys. Rev. B **30**, 6245 (1984).
[7]A. K. Sood, J. Menéndez, M. Cardona, and K. Ploog, Phys. Rev. Lett. **54**, 2115 (1985).
[8]E. Zucker, A. Pinczuk, D. S. Chemla, A. C. Gossard, and W. Wiegmann, Phys. Rev. Lett. **51**, 1293 (1983); Phys. Rev. B **29**, 7065 (1984).
[9]J. E. Zucker, A. Pinczuk, and D. S. Chemla, Phys. Rev. B **38**, 4287 (1988).
[10]A. K. Sood, J. Menéndez, M. Cardona, and K. Ploog, Phys. Rev. Lett. **54**, 2111 (1985).
[11]S. Zhang, T. A. Gant, M. Delaney, M. V. Klein, J. Klem, H. Morkoç, Chin. Phys. Lett. **5**, 113 (1988).
[12]R. Fuchs and K. L. Kliewer, Phys. Rev. **140**, A2076 (1965).
[13]W. E. Jones and R. Fuchs, Phys. Rev. B **4**, 3581 (1971).
[14]G. Kanellis, J. F. Morhange, and M. Balkanski, Phys. Rev. B **28**, 3406 (1983).
[15]S. K. Yip and Y. C. Chang, Phys. Rev. B **30**, 7037 (1984).
[16]E. Richter and D. Strauch, Solid State Commun. **64**, 864 (1987).
[17]Shanf-Fen Ren, Hanyou Chu, and Y. C. Chang, Phys. Rev. Lett. **59**, 1841 (1987).
[18]Kun Huang and Bangfen Zhu, Phys. Rev. B **38**, 2183 (1988); **38**, 13 377 (1988); Bangfen Zhu, *ibid.* **38**, 7694 (1988).
[19]E. Zucker, A. Pinczuk, D. S. Chemla, A. C. Gossard, and W. Wiegmann, Phys. Rev. Lett. **53**, 1280 (1984).
[20]To our knowledge, an important attempt at a systematic theoretical treatment of the subject has been made by J.E. Zucker, Ph.D. thesis, Columbia University, 1985, available from University Microfilms International, Ann Arbor, MI 48106, U.S.A.
[21]Y. C. Chang and J. N. Shulman, Appl. Phys. Lett. **43**, 536

(1983); Phys. Rev. B **29**, 1807 (1984); **31**, 2068 (1985); J. N. Shulman and Y. C. Chang, *ibid.* **31**, 2056 (1985).
[22]L. J. Sham, Superlatt. Microstruct. **5**, 335 (1989), and references therein.
[23]Bangfen Zhu and Kun Huang, Phys. Rev. B **36**, 8102 (1987).
[24]Bangfen Zhu, Phys. Rev. B **37**, 4689 (1988); **38**, 13 316 (1988).
[25]Hui Tang and Kun Huang, Chin. J. Semicond. **8**, 1 (1987).
[26]Bangfen Zhu, Kun Huang, and H. Tang, Phys. Rev. B **40**, 6299 (1989).
[27]R. Loudon, Proc. R. Soc., London, Ser. A **275**, 218 (1963).
[28]R. M. Martin, Phys. Rev. B **4**, 3676 (1971).
[29]For finite phonon dispersion, the interface modes are partially mixed with the bulklike modes with nearby frequencies, leading to different expressions for the displacement and potential of optical modes in superlattices, especially for the $z\bar{z}$ backscattering configuration, where the parallel component of the phonon wave vector, $k_{\parallel}$, is effectively vanishing, and the interface modes actually vibrate at frequencies close to the bulk phonon bands. Thus, the z displacements of LO modes, including bulklike and interface modes, will behave like sinusoidal standing waves, and the $n=1$ mode has, in fact, evolved from the interface mode.
[30]A. Alexandrou, M. Cardona, and K. Ploog, Phys. Rev. B **38**, 2196 (1988).